

Comparative study of dissolved and nanoparticulate Ag effects on the life cycle of an estuarine meiobenthic copepod, *Amphiascus tenuiremis*

Mithun Sikder, Emily Eudy, G. Thomas Chandler & Mohammed Baalousha

To cite this article: Mithun Sikder, Emily Eudy, G. Thomas Chandler & Mohammed Baalousha (2018): Comparative study of dissolved and nanoparticulate Ag effects on the life cycle of an estuarine meiobenthic copepod, *Amphiascus tenuiremis*, *Nanotoxicology*, DOI: [10.1080/17435390.2018.1451568](https://doi.org/10.1080/17435390.2018.1451568)

To link to this article: <https://doi.org/10.1080/17435390.2018.1451568>



[View supplementary material](#)



Published online: 19 Mar 2018.



[Submit your article to this journal](#)



[View related articles](#)



[View Crossmark data](#)

ARTICLE



Comparative study of dissolved and nanoparticulate Ag effects on the life cycle of an estuarine meiobenthic copepod, *Amphiascus tenuiremis*

Mithun Sikder^{a,b}, Emily Eudy^{a,b}, G. Thomas Chandler^{a,b} and Mohammed Baalousha^{a,b}

^aSouth Carolina SmartState Center for Environmental Nanoscience and Risk (CENR), Arnold School of Public Health, University of South Carolina, Columbia, SC, USA; ^bDepartment of Environmental Health Sciences, Arnold School of Public Health, University of South Carolina, Columbia, SC, USA

ABSTRACT

Many nanotoxicological studies have assessed the acute toxicity of nanoparticles (NPs) at high exposure concentrations. There is a gap in understanding NP chronic environmental effects at lower exposure concentrations. This study reports life-cycle chronic toxicity of sublethal exposures of polyvinylpyrrolidone-coated silver nanoparticles (PVP-AgNPs) relative to dissolved silver nitrate (AgNO_3) for the estuarine meiobenthic copepod, *Amphiascus tenuiremis*, over a range of environmentally relevant concentrations, i.e., 20, 30, 45, and $75 \mu\text{g}\text{-Ag L}^{-1}$. A concentration-dependent increase in mortality of larval nauplii and juvenile copepodites was observed. In both treatment types, significantly higher mortality was observed at 45 and $75 \mu\text{g}\text{-Ag L}^{-1}$ than in controls. In AgNO_3 exposures, fecundity declined sharply (1.8–7 fold) from 30 to $75 \mu\text{g}\text{-Ag L}^{-1}$. In contrast, fecundity was not affected by PVP-AgNPs exposures. A Leslie matrix population-growth model predicted sharply 60–86% of decline in overall population sizes and individual life-stage numbers from 30–75 $\mu\text{g}\text{-Ag L}^{-1}$ as dissolved AgNO_3 . In contrast, no population growth suppressions were predicted for any PVP-AgNPs exposures. Slower release of dissolved Ag from PVP-AgNPs and/or reduced Ag uptake in the nanoform may explain these sharp contrasts in copepod response.

ARTICLE HISTORY

Received 14 January 2018
Revised 8 March 2018
Accepted 9 March 2018

KEYWORDS

Silver nanoparticles; dissolved silver; chronic exposure; nanotoxicity; sublethal effect; life-cycle toxicity test; reproductive effects; population growth model; meiobenthos

Introduction

Ever increasing commercial application of engineered nanoparticles (NPs) has led to currently >1800 nano-enabled products in the consumer market, 438 of which contain silver nanoparticles (AgNPs; Vance et al. 2015). Environmental hazards to aquatic ecosystems are on the rise from episodic release of AgNPs from industrial, consumer, and medical products (Abbasi et al. 2016; Wei et al. 2015; Franci et al. 2015). Expected environmental concentrations of AgNPs based on modeling approaches – in the aquatic environment (i.e. surface water and sewage treatment effluent) – are estimated between $0.1 \text{ ng}\text{-Ag L}^{-1}$ and $0.1 \mu\text{g}\text{-Ag L}^{-1}$ (Gottschalk, Kost, and Nowack 2013). Thus, there is a need for better understanding of AgNPs behaviors and effects at environmentally realistic low concentrations. Past eco-toxicological studies have focused on acute AgNP toxicity to bacteria (Gunsolus et al. 2015), algae (Sørensen and Baun

2015; Navarro et al. 2015), cladocerans (Newton et al. 2013; Stensberg et al. 2014), fish (Kim et al. 2013; Kwok et al. 2016), aquatic plants (Cox et al. 2016), estuarine polychaete (Cong et al. 2014), and cell lines (Yue et al. 2015; Ivask et al. 2014; Yue et al. 2016). Many studies have demonstrated AgNP-associated lethality, reproductive failures, and embryonic development failures. Consistently, several studies have noted that AgNPs toxic effects might be due to NP dissolution and release of ionic silver (Choi and Hu 2008; Stensberg et al. 2014). However, most of these studies employed high AgNPs concentrations (e.g. $\text{mg}\text{-Ag L}^{-1}$) with far less than life-cycle exposure times for most multicellular models. Furthermore, few studies have measured chronic toxicity under low concentrations (e.g. $\mu\text{g}\text{-Ag L}^{-1}$) for AgNPs and other NPs (Zhu et al. 2008; Hoecke et al. 2009; Templeton et al. 2006), where dissolution behaviors might be different (Baalousha et al. 2016).

CONTACT Mohammed Baalousha  mbaalous@mailbox.sc.edu  Department of Environmental Health Sciences, University of South Carolina, 921 Assembly Street, Columbia, SC 29208, USA

 Supplemental data for this article can be accessed [here](#).

© 2018 Informa UK Limited, trading as Taylor & Francis Group

The meiobenthos, a group of short-lived microinvertebrates, has gained attention as a useful collection of species for chronic bioassay of environmentally realistic sediment and waterborne contaminants over life cycle (Lotufo 1997; Dahl, Gorokhova, and Breitholtz 2006; Breitholtz and Wollenberger 2003). Meiobenthic copepods such as *Amphiascus tenuiremis* serve as a predominant food source for juvenile fishes, shrimps, and crabs (Coull 1990; Gee 1989) and are often the most sensitive meiobenthic taxon to pollution (Coull and Chandler 1992). Since, *A. tenuiremis* is at the base of the food web in estuarine ecosystems, changes in its population quantity or quality may result in population changes of other dependent fauna.

The aims of this study were to (1) determine and compare the life-cycle developmental and reproductive response of the model estuarine meiobenthic copepod, *A. tenuiremis*, to chronic $\mu\text{g}\text{-Ag L}^{-1}$ levels of polyvinylpyrrolidone-coated silver nanoparticles (PVP-AgNPs) and dissolved Ag using aqueous-renewal microplate-based life-cycle toxicity test (ASTM 2012) and (2) predict/compare multigenerational effects at the population-growth level using empirical life-table data collected from each toxicity test.

Materials and methods

Chemicals

All glassware used for AgNP synthesis was washed with 10% of nitric acid followed by thorough washing using ultrahigh purity water (18.2 M Ω cm). Ninety-nine percentage of pure sodium citrate ($\text{Na}_3\text{C}_6\text{H}_5\text{O}_7$) supplied by VWR (West Chester, PA), 99.9% of pure silver nitrate (AgNO_3) and greater than 98% of pure sodium borohydride (NaBH_4) supplied by Alfa Aesar (Ward Hill, MA), and 99% of pure polyvinylpyrrolidone (PVP) of molecular weight 10,000 supplied by Sigma-Aldrich (St. Louis, MO) were used for synthesis of AgNPs. Trace metal grade nitric acid (68–70% HNO_3) supplied by Fisher Scientific (Hampton, NH) was used to acidify samples for inductively coupled plasma-mass spectroscopy (ICP-MS) analysis. Indium (supplied by PerkinElmer Internal Standard Mix, Shelton, CT) was used as internal standard for ICP-MS analysis and ARISTAR PLUS silver (Ag) standard manufactured by British Drug House (BDH Chemicals, Radnor, PA) was used

to prepare standards for ICP-MS calibration. Crystal SeasTM bioassay grade synthetic seawater (SSW) was purchased from Instant Ocean[®] (Marine Enterprises International, Baltimore, MD) and the composition of SSW is given in Table S1.

Synthesis of PVP-AgNPs

Citrate-coated precursor AgNPs (cit-AgNPs) were first synthesized by reduction of Ag^+ ions using NaBH_4 as a reducing agent and citrate as a capping agent (Romer et al. 2011). Briefly, 100 mL of 0.31 mM $\text{Na}_3\text{C}_6\text{H}_5\text{O}_7$, 100 mL of 0.25 mM AgNO_3 , and 10 mL of 0.25 mM sodium borohydride were prepared in ultra-high purity water (18.2 M Ω cm) and kept in darkness at 4°C for 30 min. AgNO_3 and $\text{Na}_3\text{C}_6\text{H}_5\text{O}_7$ solutions were stirred in a flask at 700 rpm (50 g) for 10 min. After that, 6 mL of NaBH_4 was added and the resulting mixture was heated for 90 min at 115°C while stirring at 350 rpm (12 g). The resulting AgNP suspension was left overnight at room temperature to cool. Cit-AgNPs were then washed using ultrafiltration (Amicon, 1 kDa regenerated cellulose membrane, Millipore, Billerica, MA) to remove excess reagents. Two hundred milliliter of resulting cit-AgNP suspension was cleaned using pressurized stirred ultrafiltration cell (Amicon, 1 kDa regenerated cellulose membrane, Millipore) to remove excess reagents before use. AgNP suspension volume was reduced to 100 ml and then replenished using 100 ml of 0.31 mM $\text{Na}_3\text{C}_6\text{H}_5\text{O}_7$ solution. This process was repeated three times to ensure removal of the majority of remaining dissolved Ag. PVP-AgNPs were obtained by ligand exchange of the cit-AgNPs precursor (Tejamaya et al. 2012). Briefly, 200 mL of cit-AgNPs was converted into PVP-AgNPs by adding 1 mL of 1.25 mM PVP (molar mass 10 000 g/mol) solution under vigorous stirring (i.e. 700 rpm) for at least 1 h. This amount of PVP was required to obtain full surface coverage of AgNPs by PVP molecules and thereby gain full steric stabilization (Afshinnia et al. 2017). PVP coating was used in this study, because it is a nontoxic polymer widely used to sterically stabilize NPs, preventing their aggregation even at the high ionic strength of seawater, and thus eliminating any aggregation-influenced toxicity response (Lu et al. 2010; Foldbjerg et al. 2009; Blinova et al. 2013).

Characterization of AgNPs

AgNPs were characterized using a multimethod approach including surface plasmon resonance (SPR), dynamic light scattering (DLS), ICP-MS, and atomic force microscopy (AFM) (Baalousha and Lead 2012; Domingos et al. 2009; Baalousha et al. 2012a). Z-average hydrodynamic diameter and polydispersity index (PDI) of synthesized PVP-AgNPs were measured using DLS (Malvern Zetasizer Nano-ZS, Westborough, MA). Electrophoretic mobility of PVP-AgNPs was measured by laser Doppler electrophoresis (Malvern Zetasizer Nano-ZS, Westborough, MA), which was used to calculate the zeta potential using Smoluchowski's assumption (Baalousha et al. 2012b). SPR spectra of PVP-AgNPs aliquots were recorded over 200–800 nm using a UV-vis spectrometer (UV 2600, Shimadzu Co., Kyoto, Japan) and a 10 cm path-length quartz cuvette. All measurements were performed in triplicate.

AFM (Cypher ES™ AFM, Asylum Research, Santa Barbara, CA) was used to measure the height (core size) and size evolution of PVP-AgNPs over 72 h in 30 ppt Crystal Seas™ bioassay grade SSW. AFM samples were prepared by depositing a drop of PVP-AgNPs suspension on freshly cleaved mica substrates for 20 min, followed by thorough washing with UHPW to avoid salt crystallization and NP aggregation (Baalousha, Prasad, and Lead 2014). AFM analyses were carried out in true noncontact mode under ambient conditions. All images were recorded in ACAirTopography mode with 256×256 pixel size resolution and a scan rate of 1.0 Hz. At least five different areas on each substrate were analyzed and a minimum of five images from each area were collected, resulting in at least 25 images for height analysis on each substrate. At least 140 height measurements were performed for each sample, which is sufficient to produce a representative and robust particle size distribution (Baalousha and Lead 2012).

Test organism

Amphiascus tenuiremis is a diosaccid harpacticoid copepod that is amphi-Atlantic in distribution ranging from the North Sea/Baltic intertidal to the southern Gulf of Mexico (Lang 1948). *A. tenuiremis* is a muddy-sediment dwelling copepod that cultures well in sediments or seawater alone under

laboratory conditions. It is a suitable test species for acute-to-life-cycle sediment or water bioassays due to its moderate acute sensitivity, high chronic sensitivity, and its small size (0.4 and 0.25 mm for females and males, respectively) (ASTM 2012). In 30 ppt SSW at 25 °C, *A. tenuiremis* passes through 12 life stages and three distinct morphologies (i.e. nauplius, copepodite, and adult), becomes reproductively competent in approximately 15 d, and has a median life time of 49 d. Adult females produce five to seven clutches per lifetime with each clutch averaging six to eight embryos in water-only culture (Green and Chandler 1996; Bejarano and Chandler 2003). All *A. tenuiremis* used in this study were obtained from laboratory sediment cultures (Chandler 1986) originally collected from a pristine muddy sediment site in the North Inlet Estuary, SC, USA.

Acute toxicity test

A 96-h acute toxicity test with adult *A. tenuiremis* was performed to determine median lethal toxicity of PVP-AgNPs and AgNO₃. Five nominal Ag concentrations (45, 75, 130, 216, and 360 µg-Ag L⁻¹) and a SSW control (30 ppt) were tested. All test glassware was washed with 10% of HCl (Fisher Scientific, Hampton, NH) and rinsed with UHPW for at least three times. SSW (30 ppt salinity; Instant Ocean®, aquarium systems, Mentor, OH) was aerated to >90% of O₂ saturation and then filtered at 0.45 µm. SSW was spiked with fully characterized PVP-AgNPs and AgNO₃ (10 mg-Ag L⁻¹ stock) in a 100-mL volumetric flask. Each treatment, including control, employed two replicates for a total of 24 polystyrene Petri dishes (Fisher Scientific, Hampton, NH). Twenty haphazardly selected adult *A. tenuiremis* were gently transferred into one Petri dish using an analytical grade Wire-Trol® glass capillary pipette (Drummond Scientific, Broomall, PA). After the transfer, overlying SSW was drawn out under microscopy using analytical grade 500-µL Hamilton® glass syringe (Hamilton, Reno, NV) so that <5 µL of SSW remained. Control (SSW) and treatment solutions (6 mL/Petri dish) were added back immediately. The Petri dishes were incubated static at 25 °C for 96 h under 12:12 h light:dark conditions. The number of dead in each Petri dish was recorded each day. At the end of the exposure period, the number of surviving copepods in each dish was counted.

These data (Figure 3(a)) were used to define a lower sublethal range of exposure concentrations (i.e. $<75 \mu\text{g-Ag L}^{-1}$) for definitive 35-d life-cycle bioassays in 96-well microplates.

96-Well microplate life-cycle toxicity test

Standardized life-cycle microplate bioassay methods (ASTM 2012; OECD 2014) were used to measure lethal and sublethal chronic responses of *A. tenuiremis* to PVP-AgNPs at $\mu\text{g L}^{-1}$ concentrations in SSW. Using the same methods, PVP-AgNPs toxicity was compared to toxicity from a positive Ag control, i.e., the soluble silver salt – AgNO_3 – dissolved SSW. Life-table data collected from each bioassay were entered into the Leslie (Lefkovich) matrix (LM) to generate comparative projections of future population abundance and population age-stage structure at the fourth filial generation under each toxicant condition (Chandler et al. 2004a). This bioassay method measures individual mean fecundity through two broods, but females of this species produce on average 5–7 broods during a mean lifetime of 49 ± 2 d (Green and Chandler 1996). Thus, LM population abundance projections presented for treatments and controls are truncated (lower) than the absolute population sizes possibly achievable by *A. tenuiremis* in the field.

Collection of test copepods

Amphiascus tenuiremis for the study were gently sieved from flow-through muddy sediment monocultures in the laboratory (Chandler 1986; OECD 2014) with 100s of adults pipetted to a 12-well Costar Netwell® microplate containing SSW and 75- μm mesh cup inserts. The inserts allowed hatching nauplii from gravid females to continuously fall ~ 3 mm to the microwell bottom over an 18–24 h period while retaining the larger adults. Captured nauplii (<18 h old) were then transferred individually to microwells of sterile 96-well ultra-low attachment polystyrene microplates (Corning Costar, Corning, NY) (ASTM 2012; OECD 2014).

Preparation of treatment solutions and microplates

For life-cycle testing, a SSW control and four lower Ag concentrations (20, 30, 45, and 75 $\mu\text{g-Ag L}^{-1}$) were prepared in SSW as described above.

Ten mg-Ag L^{-1} PVP-AgNPs and AgNO_3 measured concentrated stocks were used to spike all treatment solutions. Fifteen ultra-low-attachment (i.e. hydrophilic) polystyrene 96-well microplates (300 μL well volume) were hydrated with UHPW for 1 h, dumped, and allowed to air dry before refilling with 250 μL of 0.2 μm filtered and aerated SSW test solution. Haphazardly selected nauplii were gently transferred into microwells using analytical grade Wire-Trol® glass capillary pipette (Drummond Scientific, Broomall, PA) silanized with an air dried solution of 80%, 3%, and 1.5% of ethyl alcohol, isopropyl alcohol, and ethyl sulfate, respectively, to facilitate nonsticky naupliar transfer. After naupliar loading, overlying transferred SSW was drawn out under a stereomicroscope by analytical grade 500- μL Hamilton® glass syringe (Hamilton, Reno, NV) so that $<5 \mu\text{L}$ of SSW remained. This procedure standardized the starting test volume in each microwell, and allowed minimum dilution of the treatment solutions from the initial nauplius transfer. Treatment and control solutions (250 μL /microwell) were added back to wells within 2–5 min using Finnpipette® multichannel analytical pipette (Thermo Labsystems, Vantaa, Finland). Two microliter of fresh centrifuged 1:1:1 mixed algal cell ($\sim 2 \times 10^7$ cells/mL) suspension of *Isochrysis galbana*, *Dunaliella tertiolecta*, and *Rhodomonas* sp. was then added to each well using a Finnpipette® analytical pipette. Each microplate was covered and placed in a temperature regulated incubator at 25 °C with 12:12 h light:dark photo-period. Per ASTM (2012) and OECD guidelines (2014), 96 nauplii were tested over three replicate microplates for each treatment and control. Every other 12-well row was reserved for individual copepod pairing and mating within each treatment or control, usually on d 18–20 of the test. Test solutions in each microwell were aspirated and replaced under microscopy every 3 d using 250- μL Hamilton glass syringe. Care was taken to ensure that no copepods were aspirated into the syringe, and no copepods experienced desiccation stress.

Copepod rearing, pairing, and mating

Survival and development rates of *A. tenuiremis* were recorded daily in each test microwell by inverted microscopy. Copepod sex was recorded at reproductive maturity. Sexually mature males and females

were collected and haphazardly paired within each treatment as individual mating pairs – one pair per microwell. All mating microwells were then reloaded with 250 μ L of fresh control or treatment solution, and each mating pair was fed 2 μ L of algae mixture as described above. Each mating pair was checked daily for the following end points: male and female survival, mating success, days to first and second clutch hatch, days between successive clutches, and total fecundity over two clutches. For all treatments, the test terminated at d 35 or after the second clutch hatch, whichever occurred first.

Stage structured population growth model

Multigenerational population-level effects of AgNO_3 and PVP-AgNPs were estimated using empirical microplate life-cycle data fitted to a stage-structured four generation Leslie matrix model (RAMAS[®] EcoLab 2.0, Applied Biomathematics, Setauket, NY) (Leslie 1945; Ferson, Ginzburg, and Silvers 1989; Power and Power 1995). A five life-stage (nauplius: copepodite:virgin-male:virgin-female:gravid female) matrix model projected population changes through four generations in each treatment or control based on (1) stage-specific survival and next stage transition rates, (2) proportions of copepodites developing into males or females (thereby capturing sex ratio shifts), (3) proportions of females able to become gravid and produce two viable clutches, and (4) fecundity (i.e. number of hatched nauplii per mating pair) through two clutches. Population projections were compared and presented relative to each within-experiment control response rather than as absolute abundance differences across AgNO_3 and PVP-AgNPs exposures. Treatment-specific instantaneous rates of population increase (λ) also were calculated for each treatment and control population. At $\lambda=1$ replacements equal losses. Thus, population size is projected stable and neither increasing nor decreasing over time.

Transformations of PVP-AgNPs in SSW

For PVP-AgNPs and AgNO_3 life-cycle toxicity tests, control and treatment solution samples were collected in triplicate at test initiation and at each renewal period (every 3 d, from microwells). Dissolved Ag species were separated from PVP-AgNPs using centrifugal ultrafiltration (3KDa

regenerated cellulose membranes, Amicon Ultra-4) at 3250 g for 15 min. The original (total Ag) and ultrafiltered (dissolved Ag) samples were acidified to 10% of HNO_3 and then diluted 200 fold in 1% of HNO_3 prior to ICP-MS (NexIONTM 350 D, PerkinElmer Inc., Waltham, MA) analysis to minimize matrix effects and avoid salt precipitation. Indium (analytical grade, BDH[®], VWR International LLC, PA) was used as an internal standard to correct for nonspectral interferences during analysis (Vanhaecke et al. 1992).

Additional experiments were conducted to quantify Ag sorption onto the microplates and onto algal food cells. Twenty and 75 $\mu\text{g}\text{-Ag L}^{-1}$ (i.e. lowest and highest exposures of the life-cycle test) as AgNO_3 or PVP-AgNPs were added to microwells without copepods and algae, followed by sample collection at 0, 24, 48, and 72 h. Sorption of Ag on algal cells was investigated by mixing 20 and 75 $\mu\text{g}\text{-Ag L}^{-1}$ (as AgNO_3 or PVP-AgNPs) with algae in 100-mL Erlenmeyer flasks at the same concentrations that were given to copepods as food followed by serial SSW sample collection at spaced time points (e.g. 0–72 h). Dissolved Ag in SSW was separated from PVP-AgNPs by centrifugal ultrafiltration. Total and dissolved Ag concentrations were then measured using ICP-MS following sample treatment as described above. All samples and analyzes were performed in triplicate.

Statistical analysis

All statistical analyses were performed with SAS[®] version 9.4 software (SAS Institute, Cary, NC). The following dependent variable means were tested for statistical significance: stage-specific survival, development rates, and percent of females becoming gravid (fertility), and brood size through two clutches (fecundity). Copepod survival, percent gravid, and offspring production within treatments and microplates were analyzed using general linear model (GLM) nested ANOVA and Tukey's multiple comparison tests. Statistical significance was set at $p < 0.05$.

Results and discussion

PVP-AgNPs characterization and transformation in SSW

The total and dissolved Ag concentrations in the PVP-AgNPs stock suspension were 11.5 ± 0.08 and

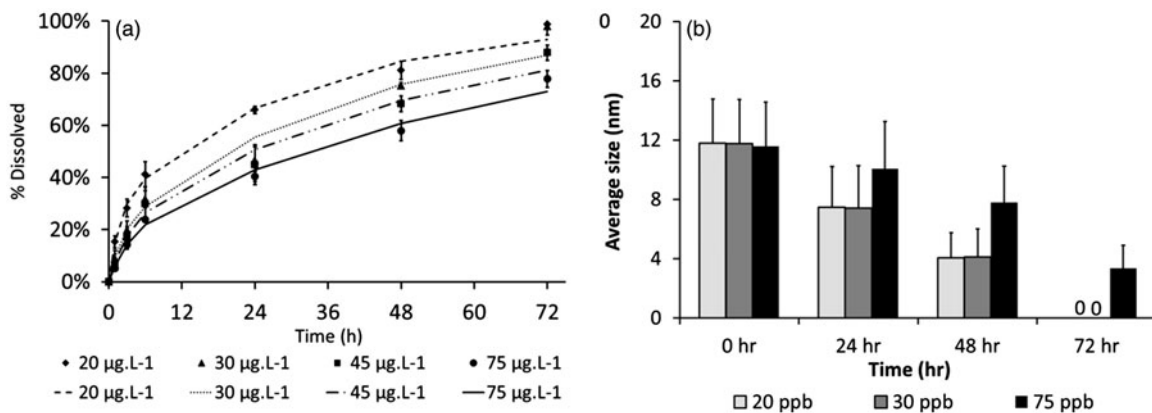


Figure 1. Behavior of polyvinylpyrrolidone-coated silver nanoparticles (PVP-AgNPs) in 30 ppt synthetic seawater (SSW): (a) % dissolved Ag measured by ICP-MS following centrifugal ultrafiltration as a function of time and (b) average NP size measured by AFM as a function of time after mixing 20, 30, 45, and 75 µg L⁻¹ PVP-AgNPs with SSW.

$0.45 \pm 0.03 \text{ mg-Ag L}^{-1}$, respectively. AFM micrographs show randomly distributed PVP-AgNPs on the mica substrate with no aggregated particles (Figure S1), indicating good sample preparation quality and good dispersion of synthesized PVP-AgNPs in UHPW (Baalousha and Lead 2012). The number-weighted PVP-AgNPs particle height measured by AFM was approximately $11.3 \pm 3 \text{ nm}$, with a height distribution range predominantly (>81%) between 8 and 14 nm (Figure S1(b)). The Z-average (intensity-weighted) hydrodynamic diameter measured by DLS was $21.6 \pm 0.3 \text{ nm}$. The larger Z-average hydrodynamic diameter compared to the particle height measured by AFM can be attributed to the higher light scattering intensity from larger particles resulting in a bias toward larger sizes (Baalousha and Lead 2012). The zeta potential of synthesized PVP-AgNPs was $-9.6 \pm 1.1 \text{ mV}$.

The initial mean PVP-AgNPs particle heights in UHPW and SSW ($11.7 \pm 3 \text{ nm}$ and $12 \pm 3 \text{ nm}$, respectively) were not significantly different (two-tailed *t*-test, $p > 0.48$). UV-vis SPR spectra of PVP-AgNPs in UHPW and SSW exhibited a characteristic absorption maximum at 404 nm (Figure S2(a, b)) without peak, suggesting that PVP-AgNPs remain colloidally stable (i.e. do not aggregate) and do not undergo shape transformation in our SSW (Baalousha et al. 2016; Sikder et al. 2017; Afshinnia et al. 2016). However, PVP-AgNPs did dissolve in SSW in a concentration-dependent manner (Figure 1(a)); i.e., PVP-AgNPs dissolved at a higher rate and to a greater extent as initial NPs concentrations decreased (Sikder et al. 2017; Baalousha et al. 2016). At low concentrations (e.g. 20 and 30 µg-Ag L⁻¹ NPs),

PVP-AgNPs dissolved completely (>98%) within 72 h; whereas at higher concentrations (e.g. 45 and 75 µg-Ag L⁻¹) 88% and 78% of NPs mass, respectively, dissolved over 72 h. The dissolution of PVP-AgNPs also resulted in a decrease in particle height (size) over time (Figures 1(b) and S3). PVP-AgNPs particle size distribution shifted toward smaller sizes and narrower size distributions (Figure S3). At 72 h, PVP-AgNPs were not detected at low NP concentrations, which is in agreement with complete dissolution as supported by ICP-MS analysis. These findings suggest that exposure to PVP-AgNPs in SSW is dynamic with variable NP and dissolved ion concentrations, and NP sizes changing over time.

Acute 96-hour exposure effects

For AgNO₃ exposures, measured mean Ag concentrations were $42.5 \pm 3.1 \text{ } \mu\text{g-Ag L}^{-1}$, $80.5 \pm 2.4 \text{ } \mu\text{g-Ag L}^{-1}$, $139.9 \pm 2.2 \text{ } \mu\text{g-Ag L}^{-1}$, $217.3 \pm 3.9 \text{ } \mu\text{g-Ag L}^{-1}$, and $351.4 \pm 6.8 \text{ } \mu\text{g-Ag L}^{-1}$ respectively for the nominal target concentrations of 45, 75, 130, 216, and 360 µg-Ag L⁻¹ (Figure S4(a)). Baseline $4.3 \pm 0.2 \text{ } \mu\text{g-Ag L}^{-1}$ was measured in control treatment during acute exposures. As measured Ag concentrations were $\geq 93\%$ of nominal targets for AgNO₃, exposure concentrations are reported on a nominal basis. Similarly, in PVP-AgNPs exposures, measured Ag concentrations were $49.1 \pm 3.8 \text{ } \mu\text{g-Ag L}^{-1}$, $77.9 \pm 4.5 \text{ } \mu\text{g-Ag L}^{-1}$, $138.7 \pm 2.6 \text{ } \mu\text{g-Ag L}^{-1}$, $217.5 \pm 5.3 \text{ } \mu\text{g-Ag L}^{-1}$, and $355 \pm 7.1 \text{ } \mu\text{g-Ag L}^{-1}$ for the same nominal targets (i.e. $\geq 91\%$ of nominal targets, Figure S4(a)). Thus, PVP-AgNPs also are reported nominally.

All water quality parameters (e.g. salinity, pH, and dissolved oxygen) met American Society of Testing and Materials (ASTM 2014) guidelines for the acute exposure test. During the acute exposure (Figure S10), control mortality was less than 10%. AgNO_3 and PVP-AgNPs were toxic to *A. tenuiremis* at or above $75 \mu\text{g L}^{-1}$ (Figure S10), with significantly higher acute toxicity for AgNO_3 (96 h, $\text{LC50} = 64.8 < 72.8 < 80.2 \mu\text{g-Ag L}^{-1}$) compared to PVP-AgNPs (96 h $\text{LC50} = 95.2 < 106.8 < 118.4 \mu\text{g-Ag L}^{-1}$). Previous tests with the planktonic copepod *Acartia tonsa* reported a 48-h LC50 of $43 \mu\text{g-Ag L}^{-1}$ for dissolved Ag in the same order of magnitude as our present 96-h finding (Hook and Fisher 2001).

The toxicity of AgNPs has been attributed to the NPs directly, or the release of Ag^+ from AgNPs dissolution, or both (Fabrega et al. 2009; Navarro et al. 2008; Griffitt et al. 2008). In this study, the observed differences in the toxicological outcomes for AgNO_3 and AgNPs can be attributed to the dynamic nature of the exposure. For AgNO_3 treatments, copepods were exposed to the maximal Ag exposure concentration (as dissolved Ag) from the beginning of the test to the end. For PVP-AgNPs treatments, copepods were exposed to a combination of intact PVP-AgNPs and dissolved Ag released from PVP-AgNPs. Thus, for PVP-AgNPs treatments, copepods were exposed for shorter times and/or to lower amounts of the most biologically active/bio-available dissolved Ag over the 96-h exposure (Croteau et al. 2011). Such differences in the nature of the full exposure regime could explain the sharply higher acute toxicity of AgNO_3 relative to PVP-AgNPs.

Chronic life-cycle exposure effects

PVP-AgNP behavior in the bioassay environment

Total Ag concentrations in SSW were measured using ICP-MS at each of 10 water changes during the AgNO_3 and PVP-AgNPs copepod life-cycle tests. Low Ag concentrations of $4.3 \pm 0.6 \mu\text{g-Ag L}^{-1}$ and $4.8 \pm 1.0 \mu\text{g-Ag L}^{-1}$ were measured in control for the AgNO_3 and PVP-AgNPs experiments, respectively. At time-zero in AgNO_3 exposures, measured total Ag concentrations ($20 \pm 2.3 \mu\text{g-Ag L}^{-1}$, $30 \pm 2.4 \mu\text{g-Ag L}^{-1}$, $46.1 \pm 4.3 \mu\text{g-Ag L}^{-1}$, and $78.1 \pm 1.5 \mu\text{g-Ag L}^{-1}$) were $\geq 94\%$ of nominal target concentrations (i.e. 20, 30, 45, 75 $\mu\text{g-Ag L}^{-1}$, Figure S4(b)). In

PVP-AgNPs exposures, measured total Ag concentrations at time-zero ($22.3 \pm 2.7 \mu\text{g-Ag L}^{-1}$, $31.4 \pm 3.5 \mu\text{g-Ag L}^{-1}$, $46.1 \pm 4.5 \mu\text{g-Ag L}^{-1}$, and $73.3 \pm 3.3 \mu\text{g-Ag L}^{-1}$) were $\geq 87\%$ of same nominal targets (Figure S4(b)). Thus, results are presented with nominal concentrations.

At the end of each 72-h renewal period, dissolved Ag concentrations measured in microwells containing algae and copepods were sharply lower for AgNO_3 (only 5–10% initial concentrations) and PVP-AgNPs (15–20% initial) (Figure S5) compared to Ag concentrations in the absence of algae and copepods (Figure 2). These low dissolved Ag concentrations at 72 h may be attributed to: (1) sorption of dissolved Ag on microplate well walls, (2) sorption of dissolved Ag on algal cells, and/or (3) Ag bioaccumulation by growing copepods. To explore these questions, we conducted additional experiments.

First, 20 and $75 \mu\text{g-Ag L}^{-1}$ (i.e. lowest and highest exposures in life-cycle test) as AgNO_3 and PVP-AgNPs were added to 30 ppt SSW in microplate microwells (without copepods and algae) followed by sample collection at 0, 24, 48, and 72 h. Approximately, 90–95% added Ag was recovered from microplates (Figure S6(a,b)) and total Ag concentrations (at 0 h) were not significantly different ($p > 0.97$) compared to recovered dissolved Ag (after 72 h). These results confirm the absence of Ag losses in the low-adsorption hydrogel-coated microwell. For PVP-AgNPs, the percent dissolved Ag concentration increased with time in organism-free microwells (Figure S6(c,d)) due to NP dissolution. Dissolution behavior of PVP-AgNPs in microplates was similar to that in batch experiments (Figure 1(a)) indicating that the low-adsorption microwell environment *per se* has no impact on PVP-AgNP dissolution behavior.

Second, to evaluate the impact of algae on dissolved Ag concentrations, 20 and $75 \mu\text{g L}^{-1}$ AgNO_3 and PVP-AgNPs were added to microwells loaded with $2 \mu\text{L}$ algae (2×10^4 cells) in SSW under the same exposure but using finer time-sampling conditions. For the $20 \mu\text{g-Ag L}^{-1}$ AgNO_3 exposure, $>90\%$ of total dissolved Ag associated with algae within 30 min (Figure S7). For the $75 \mu\text{g-Ag L}^{-1}$ AgNO_3 exposure, 59% of dissolved Ag associated with algae within 30 min and then increased to $>90\%$ Ag by 72 h (Figure S7). Similarly, for PVP-AgNPs,

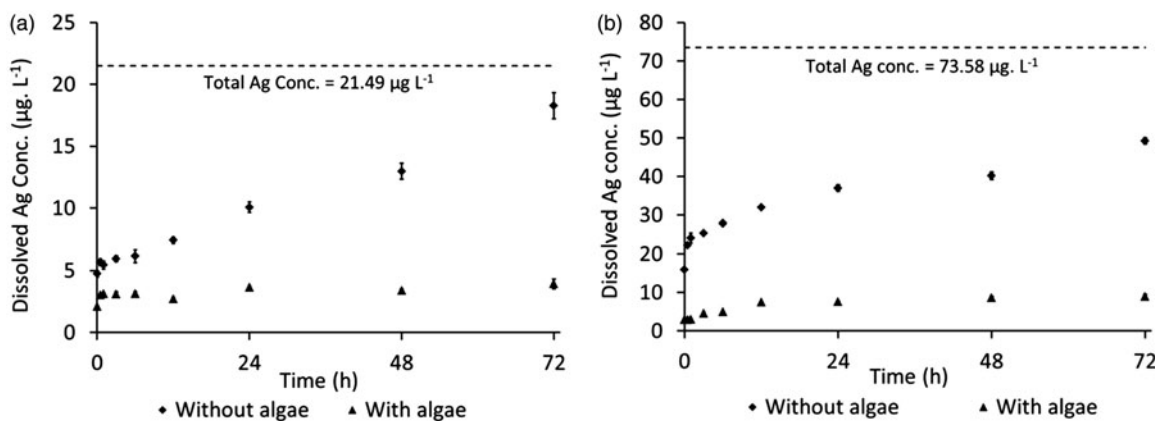


Figure 2. Dissolved Ag concentration (<3 kDa) as a function of time following mixing at (a) 20 µg L⁻¹ and (b) 75 µg L⁻¹ polyvinylpyrrolidone-coated silver nanoparticles (PVP-AgNPs) with 30 ppt SSW in presence and absence of algae.

dissolved Ag in microwells represented <20% of the total Ag released by PVP-AgNPs dissolution over the 72 h renewal period (Figure 2(a,b)). For both the 20 and 75 µg-Ag L⁻¹ NP exposures, Ag sorption on algae was rapid (Figure 2) and dissolved Ag decreased with time in the solution phase. After 72 h, only 3.7 and 8.4 µg-Ag L⁻¹ respectively remained in solution at 20 and 75 µg-Ag L⁻¹ PVP-AgNPs.

Copepod survival and development rates in chronic life-cycle exposures. Development of the most sensitive naupliar copepod life-stage was normal in all Ag-free controls with an overall control mortality $\leq 10\%$ (Figure 3(b)). Naupliar mortalities in the 20 and 30 µg-Ag L⁻¹ treatments (for both AgNO₃ and PVP-AgNPs) were also $\leq 10\%$. However, significantly higher naupliar mortality was seen at 45 and 75 µg-Ag L⁻¹ ($p < 0.05$). Both AgNO₃ and PVP-AgNPs produced a concentration-dependent increase in naupliar and copepodite mortality that peaked at 34% and 23% death, respectively (Figure 3(b,c)). As this bioassay is focused on measuring sublethal life-cycle effects, test concentrations were set to achieve ideally $\leq 30\%$ maximum naupliar mortality. This condition was largely met. The highest 75 µg-Ag L⁻¹ exposure to AgNO₃ and PVP-AgNPs yielded only 23.8% and 17.7% naupliar mortality, respectively. AgNO₃ showed consistently higher naupliar mortality than PVP-AgNPs in most treatments, but cross-treatment differences were significant only at 45 µg-Ag L⁻¹ ($p < 0.05$). AgNO₃ and PVP-AgNPs exposures produced lower, but similar ($p > 0.05$) mortality patterns (Figure 3(c)) across the treatment concentration range for the less sensitive juvenile copepodite stage.

Nauplius-to-copepodite development rates (i.e. days to copepodite; Figure S8(a)) were not significantly different across treatments and control, except at 75 µg-Ag L⁻¹ PVP-AgNPs, which was delayed by 2 d ($p < 0.05$). For the copepodite-to-adult development window, no significant effect of Ag in either form was observed (Figure S8(b)).

Overall, these results show that larval nauplii are the most sensitive copepod life-stage to Ag generally. Based on naupliar mortality patterns, repeated 72-h exposures to dissolved AgNO₃ were more toxic than repeated exposures to PVP-AgNPs. However, juvenile-stage copepodite mortality and development rates (i.e. copepodite-to-adult) were not significantly different between Ag treatments.

Reproductive effects. The number of adult mating pairs able to produce viable offspring through ≥ 18 d of mating was significantly reduced in 30 and 75 µg-Ag L⁻¹ AgNO₃ treatments relative to controls ($p < 0.05$, Figure 4). Reproductive success is defined as proportion of females in each treatment able to produce at least two viable clutches of offspring in ≤ 35 d. The 30 and 75 µg-Ag L⁻¹ AgNO₃ treatments showed 55% and 81% lower mating success, respectively, while 20 and 45 µg-Ag L⁻¹ AgNO₃ treatments showed decreases of 23% and 25% relative to controls ($\geq 67\%$ successful; Figure 4). Note that higher AgNO₃ concentrations (e.g. 45 and 75 µg-Ag L⁻¹) led to low n-sizes of only four and two mating pairs respectively due to high lifetime copepod mortality. Because of these low n-sizes no statistical inferences can be made regarding actual mating success at these concentrations. For those surviving females able to reproduce, the time

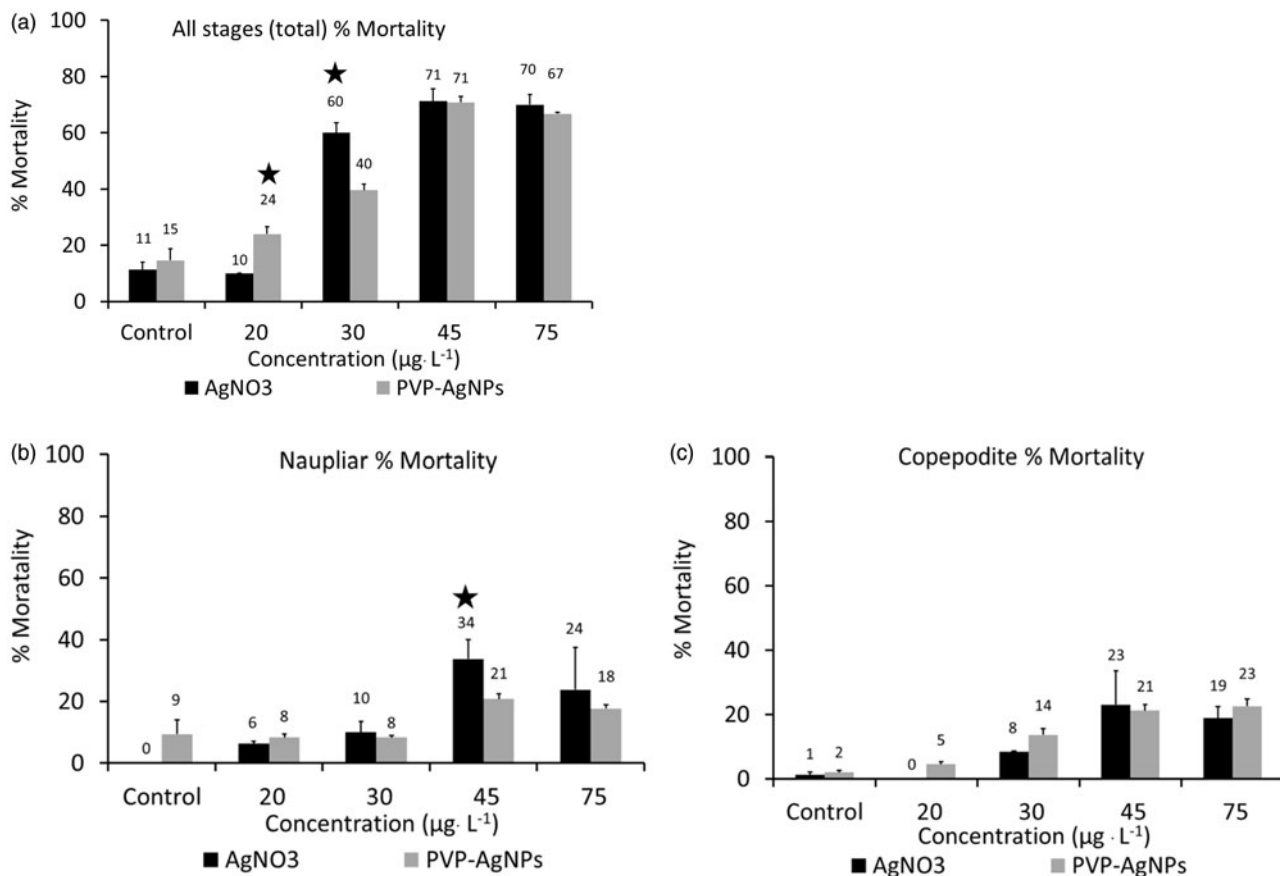


Figure 3. (a) All stages (total) mortality, (b) Naupliar mortality, and (c) copepodite (juvenile) mortality in sub-lethal life-cycle exposure to silver nitrate (AgNO_3) and polyvinylpyrrolidone-coated silver nanoparticles (PVP-AgNPs) (* indicates statistically significant difference between mean responses within a given Ag-treatment concentration; $p < 0.05$).

required to extrude/hatch two brood sacs was delayed significantly by 2.5 and 3.3 d respectively at 45 and $75 \mu\text{g}\cdot\text{Ag L}^{-1}$ AgNO_3 ($p < 0.05$, Figure 5). In contrast to AgNO_3 , mating success in PVP-AgNPs treatments was not significantly different from controls at any concentration ($p > 0.37$, Figure 4), and no significant delays in brood sac extrusions/hatch occurred ($p > 0.1$, Figure S9).

Mean fecundity was calculated as the average number of hatched offspring through two broods per successful mating pair in ≤ 35 d. Increasing AgNO_3 concentrations produced a consistent trend of depressed fecundity (19–40% lower) compared to the control ($p < 0.05$, Figure 6). In sharp contrast, PVP-AgNPs had no significant effects on fecundity at any concentration ($p > 0.27$, Figure 6), even though Ag was liberated freely by PVP-NPs dissolution over the exposure period.

Stage-structured Leslie matrix population growth models. The microplate culturing approach allows life-cycle tracking of each individual's survival,

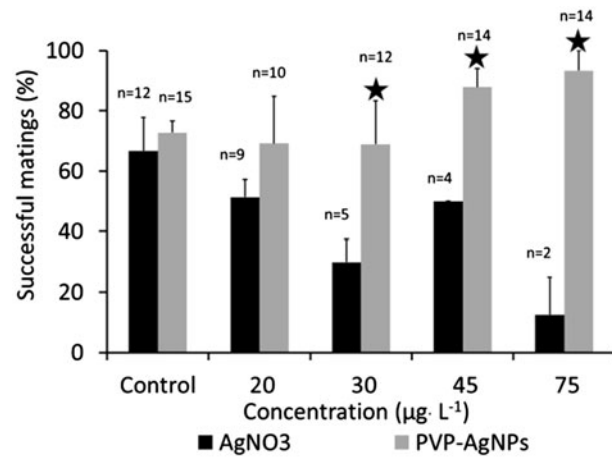


Figure 4. Percent of females able to produce two broods of viable offspring over 18–24 d of mating (n-sizes vary across treatments/concentrations depending on survival rates of nauplii to sexually mature adults; * indicates significant difference between mean responses within a given Ag-treatment concentration; $p < 0.05$).

development, sex, fertility, and reproductive output (fecundity). These endpoints allow population-level responses to be predicted over time via a

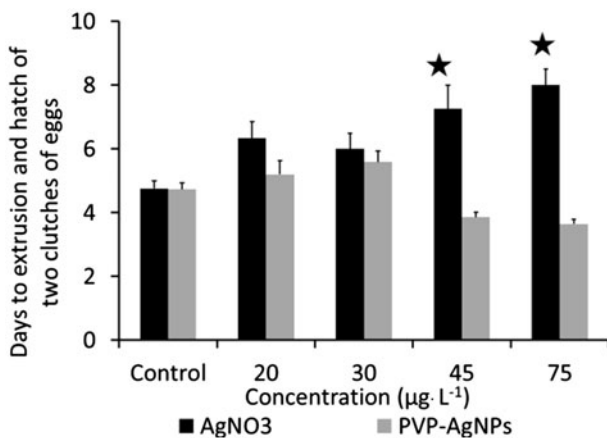


Figure 5. Time to extrusion and hatch of two clutches of eggs in silver nitrate (AgNO_3) and polyvinylpyrrolidone-coated silver nanoparticles (PVP-AgNPs) treatments (*indicates significantly delayed extrusion compared to control treatment; $p < 0.05$).

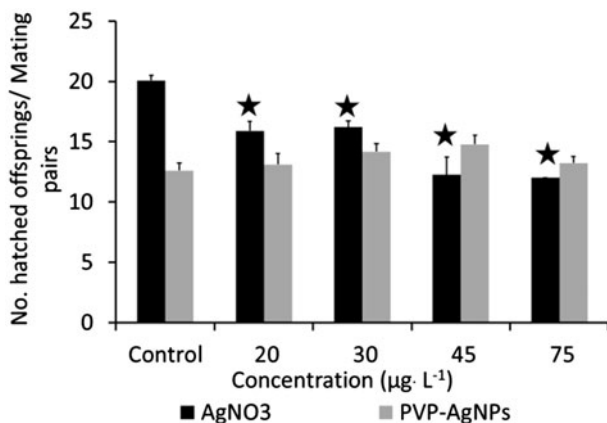


Figure 6. Number of hatched offspring through two broods per mating pair (mean fecundity) in silver nitrate (AgNO_3) and polyvinylpyrrolidone-coated silver nanoparticles (PVP-AgNPs) treatments (* indicates significantly reduced number of hatched offspring compared to control; $p < 0.05$).

life-stage-based adaptation of the LM population growth model (Leslie 1945; Power and Power 1995; Ferson, Ginzburg, and Silvers 1989). LM models also predict finite rates of population increase (λ , instantaneous growth rate) based on same measured stage-specific mortality, sexual development, and reproductive endpoints (Chandler et al. 2004b). A λ of unity implies a population is neither growing nor declining. A value less than unity implies population decline, and greater than unity implies population growth. AgNO_3 λ s ranged from 0.76 for the highest 75 $\mu\text{g}\cdot\text{L}^{-1}$ treatment to 1.21 for the lowest 20 $\mu\text{g}\cdot\text{L}^{-1}$ treatment. The instantaneous growth rate for the AgNO_3 control population was 1.24, but the 30 and 75 $\mu\text{g}\cdot\text{L}^{-1}$ treatment data

Table 1. Leslie matrix predicted instantaneous population growth rate (λ) of *Amphiascus tenuiremis* in presence of silver nitrate (AgNO_3) and polyvinylpyrrolidone-coated silver nanoparticles (PVP-AgNPs).

Exposure concentration ($\mu\text{g}\cdot\text{L}^{-1}$)	Population growth rate (λ)	
	AgNO_3 exposure	PVP-AgNPs exposure
Control	1.24	1.26
20	1.21	1.25
30	0.89	1.29
45	1.01	1.18
75	0.76	1.17

predicted sharply reduced growth rates (Table 1). In contrast, all PVP-AgNPs copepod populations had λ s in strong excess of unity and similar to Ag -free controls. The highest 45 and 75 $\mu\text{g}\cdot\text{L}^{-1}$ treatments showed mildly suppressed λ s relative to controls, but both were well-above ‘no-growth’ unity (Table 1).

A λ provides a single-digit rate estimation of potential population growth, but the Leslie matrix gives multigenerational projections of copepod population size and age-stage structure for each treatment and control population at multiple future generations (e.g. four in this study) [four generations was arbitrarily chosen; see Figure 7(a)]. The 30–75 $\mu\text{g}\cdot\text{L}^{-1}$ life-table data for AgNO_3 predicted sharp decreases of 60–86% in estimated population sizes relative to the control. In contrast, the 30–75 $\mu\text{g}\cdot\text{L}^{-1}$ life-table data PVP-AgNPs predicted 2–5 times higher population sizes than for AgNO_3 , even though measured dissolved Ag in PVP-AgNPs SSW exceeded 30 $\mu\text{g}\cdot\text{L}^{-1}$ within 24 h in, e.g., the 75 $\mu\text{g}\cdot\text{L}^{-1}$ PVP-AgNPs treatment (Figure 1(a)). AgNO_3 life-table data at 30, 45, and 75 $\mu\text{g}\cdot\text{L}^{-1}$ similarly predicted sharp depressions in relative abundances of every individual copepod life-stage (Figure 7(b–d)). Relative to PVP-AgNP controls, naupliar larvae projections were depressed 9.8–77.3%, copepodite juveniles by 45.7–81.9%, adult females by 62.6–78.5%, and gravid females by 64.4–89%. In AgNO_3 , these predicted life-stage declines were primarily driven by low reproductive success (fertility and fecundity) in the bioassay. In contrast, PVP-AgNPs life-table data produced fourth-generation life-stage structures that were all similar to control structure/abundance irrespective of PVP-AgNPs concentration (Figure 7(b–d)).

A. tenuiremis survival and reproductive ability is highly sensitive to dissolved Ag concentration.

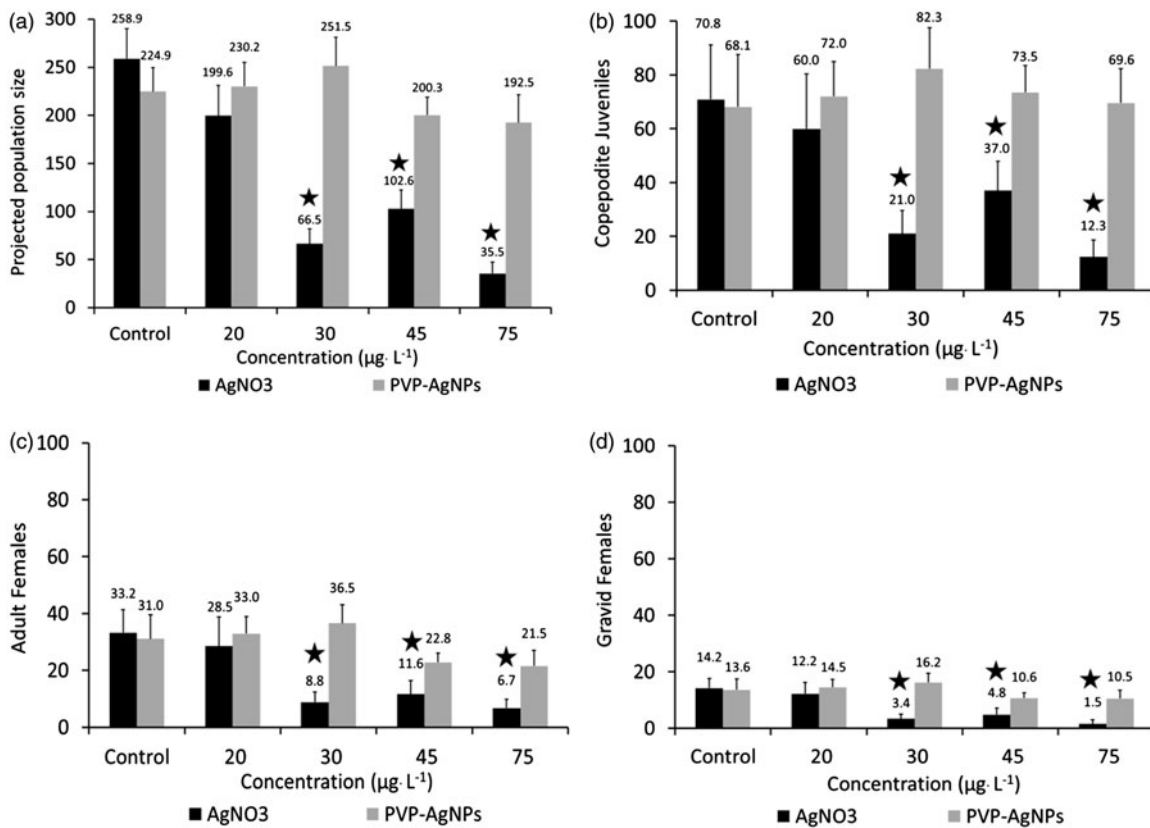


Figure 7. (a) Leslie matrix projected silver nitrate (AgNO₃) and polyvinylpyrrolidone-coated silver nanoparticles (PVP-AgNPs) impacts on *Amphiascus tenuiremis* population sizes after four generations. Each treatment-specific mean abundance represents 10,000 replications of a simulated population growth model starting with 38 nauplii, 30 copepodites, 12 males, 6 gravid, and 14 nongravid females (* indicates a significantly depressed (>2 s difference) population size relative to its within-treatment control). (b, c, and d) Final-stage abundance projections of copepodite juveniles, adult females, and gravid females after four generations of exposure (* indicates a significantly depressed (>2 s difference) life-stage abundance relative to its within-treatment control).

This is consistent with previous studies where, e.g., Ag-related reproductive, histological, and biochemical impairment of planktonic copepods (*A. tonsa*) and daphniids (*Daphnia magna*) occurred when they were fed algal food incubated in dissolved Ag (AgNO₃) at 27–108 $\mu\text{g-Ag L}^{-1}$ (0.25–1 nM) (Hook and Fisher 2001; Bielmyer, Grosell, and Brix 2006). Reduced egg numbers were observed when *A. tonsa* was fed algal food exposed to AgNO₃, and total protein concentration per egg (lipovitellin) and percentage of copepod females with developed ovaries decreased with increasing Ag ingestion (Hook and Fisher 2001). Lipovitellin is the predominant soluble egg protein (Shafir et al. 1992) in crustaceans and most invertebrates, and its accumulation in egg follicles is required for maximum egg quality and offspring survival/development (Raikhel and Dhadialla 1992). These studies demonstrate that dietary metals' assimilation efficiencies by copepods are strongly related to the metal concentrations

inside or on the surface of algal food which potentially become bioavailable during ingestion (Reinfelder and Fisher 1991; Hutchins, Wang, and Fisher 1995; Xu and Wang 2004).

Nature of the exposure: dissolved Ag vs. AgNP effects. Toxicity of AgNPs has been attributed to direct AgNPs effects, the release of Ag⁺ from AgNPs dissolution, or to both (Fabrega et al. 2009; Navarro et al. 2008; Griffitt et al. 2008). In this study, the observed differences in toxicological response for AgNO₃ versus AgNPs can be attributed to the dynamics of [Ag⁺] change over each 72-h treatment renewal period. For each AgNO₃ test concentration, copepods were exposed for 35 d to the maximal dissolved Ag concentration that could be delivered, in fresh 72-h doses, and with a significant proportion of dissolved Ag rapidly sorbed to the surfaces of algal cell food. For PVP-AgNPs treatments, the actual realized exposure is a combination of intact

PVP-AgNPs in suspension and also associated with algal food, plus any released dissolved Ag from the PVP-AgNPs' gradual dissolution and sorption to food. Hence, under similar microplate conditions, PVP-AgNPs exposures likely produced less freely dissolved Ag than AgNO_3 exposures. Thus, for PVP-AgNPs, copepods likely were exposed integratively to lower amounts of the most biologically-active dissolved Ag complexes over each 72-h microwell SSW renewal and subsequently to lower total amounts over the full 35-d test duration. This could explain the sharply lower effects of PVP-NPs (i.e. better survival, development, reproduction, and population growth potential) on *A. tenuiremis* compared to the severe chronic effects observed for dissolved AgNO_3 .

Environmental implications

Copepods are the most abundant arthropods on earth, and nearly the most abundant of all metazoans known, rivaled only by nematode round-worms (Giere 2009). For aquatic/marine ecosystems, they are a key to food-web integrity, quality, and sustainability (Hicks and Coull 1983). Impacts of contaminants on the reproductive success of an important prey species could affect the population dynamics of that species and possibly other species dependent on it through selective grazing or predation. Since, *A. tenuiremis* and other meiobenthic copepods are a key part of the diet of fishes (Gee 1989), shrimps, and crabs (Coull 1990), there is potential for Ag uptake and subsequent transfer to higher level organisms of direct value to humans.

Copepod exposure to PVP-AgNPs had little effect on their ability to survive, reproduce, and increase population size. Environmental release of AgNPs from consumer products, sewage outfalls, etc. would, however, still pose some risk to marine ecosystems through the rapid and complete dissolution of AgNPs in seawater. Therefore, researchers, policy-makers, and regulators should carefully consider unintended effects of dissolved Ag release from AgNPs when considering potential risks of AgNPs. For a more informed risk assessment of AgNPs, future studies should evaluate whether dissolved Ag and AgNPs exhibit similar reproductive and population toxicity patterns for a broader spectrum of chronically exposed invertebrate phyla. Such population-relevant

data, along with others, could be used to produce a more useful holistic model for predicting AgNPs risks to estuarine and aquatic ecosystems.

Disclosure statement

The authors report no conflicts of interest. The authors alone are responsible for the contents and writing of the paper.

Funding

This research was supported by the United States National Science Foundation [NSF1437307].

References

- Abbasi, E., M. Milani, S. Fekri Aval, M. Kouhi, A. Akbarzadeh, H. Tayefi Nasrabadi, P. Nikasa, et al. 2016. "Silver Nanoparticles: Synthesis Methods, Bio-Applications and Properties." *Critical Reviews in Microbiology* 42: 173–180.
- Afshinnia, K., I. Gibson, R. Merrifield, and M. Baalousha. 2016. "The Concentration-Dependent Aggregation of Ag NPs Induced by Cystine." *Science of the Total Environment* 557–558: 395–403.
- Afshinnia, K., M. Sikder, B. Cai, and M. Baalousha. 2017. "Effect of Nanomaterial and Media Physicochemical Properties on Ag NM Aggregation Kinetics." *Journal of Colloid and Interface Science* 487: 192–200.
- ASTM. 2012. *Standard Guide for Conducting Renewal Microplate-Based Life-Cycle Toxicity Tests with a Marine Meiobenthic Copepod*. West Conshohocken, PA: ASTM International.
- ASTM. 2014. *Standard Guide for Conducting Acute Toxicity Tests on Test Materials with Fishes, Macroinvertebrates, and Amphibians*. West Conshohocken, PA: ASTM International.
- Balousha, M., Y. Ju-Nam, P. A. Cole, B. Gaiser, T. F. Fernandes, J. A. Hriljac, M. A. Jepson, V. Stone, C. R. Tyler, and J. R. Lead. 2012a. "Characterization of Cerium Oxide Nanoparticles — Part 1: Size Measurements." *Environmental Toxicology and Chemistry* 31: 983–993.
- Balousha, M., Y. Ju-Nam, P. A. Cole, J. A. Hriljac, I. P. Jones, C. R. Tyler, V. Stone, T. F. Fernandes, M. A. Jepson, and J. R. Lead. 2012b. "Characterization of Cerium Oxide Nanoparticles — Part 2: Nonsize Measurements." *Environmental Toxicology and Chemistry* 31: 994–1003.
- Balousha, M., and J. R. Lead. 2012. "Rationalizing Nanomaterial Sizes Measured by Atomic Force Microscopy, Flow Field-Flow Fractionation, and Dynamic Light Scattering: Sample Preparation, Polydispersity, and Particle Structure." *Environmental Science & Technology* 46 (11): 6134–6142.

Baalousha, M., A. Prasad, and J. R. Lead. 2014. "Quantitative Measurement of the Nanoparticle Size and Number Concentration from Liquid Suspensions by Atomic Force Microscopy." *Environmental Science-Processes & Impacts* 16: 1338–1347.

Baalousha, M., M. Sikder, A. Prasad, J. Lead, R. Merrifield, and G. T. Chandler. 2016. "The Concentration-Dependent Behaviour of Nanoparticles." *Environmental Chemistry* 13: 1–3.

Bejarano, A. C., and G. T. Chandler. 2003. "Reproductive and Developmental Effects of Atrazine on the Estuarine Meiobenthic Copepod *Amphiascus tenuiremis*." *Environmental Toxicology and Chemistry* 22: 3009–3016.

Bielmyer, G. K., M. Grosell, and K. V. Brix. 2006. "Toxicity of Silver, Zinc, Copper, and Nickel to the Copepod *Acartia tonsa* Exposed via a Phytoplankton Diet." *Environmental Science & Technology* 40: 2063–2068.

Blinova, I., J. Niskanen, P. Kajankari, L. Kanarbik, A. Käkinen, H. Tenhu, O.-P. Penttinen, and A. Kahru. 2013. "Toxicity of Two Types of Silver Nanoparticles to Aquatic Crustaceans *Daphnia magna* and *Thamnocephalus platyurus*." *Environmental Science and Pollution Research* 20: 3456–3463.

Breitholtz, M., and L. Wollenberger. 2003. "Effects of Three PBDEs on Development, Reproduction and Population Growth Rate of the Harpacticoid Copepod *Nitocra spinipes*." *Aquatic Toxicology (Amsterdam, Netherlands)* 64 (1): 85–96.

Chandler, G. T. 1986. "High-Density Culture of Meiobenthic Harpacticoid Copepods within a Muddy Sediment Substrate." *Canadian Journal of Fisheries and Aquatic Sciences* 43: 53–59.

Chandler, G. T., T. L. Cary, A. C. Bejarano, J. Pender, and J. L. Ferry. 2004a. "Population Consequences of Fipronil and Degradates to Copepods at Field Concentrations: An Integration of Life Cycle Testing with Leslie Matrix Population Modeling." *Environmental Science & Technology* 38: 6407–6414.

Chandler, G. T., T. L. Cary, D. C. Volz, S. S. Walse, J. L. Ferry, and S. L. Klosterhaus. 2004b. "Fipronil Effects on Estuarine Copepod (*Amphiascus tenuiremis*) Development, Fertility, and Reproduction: A Rapid Life-Cycle Assay in 96-Well Microplate Format." *Environmental Toxicology and Chemistry* 23: 117–124.

Choi, O., and Z. Hu. 2008. "Size Dependent and Reactive Oxygen Species Related Nanosilver Toxicity to Nitrifying Bacteria." *Environmental Science & Technology* 42: 4583–4588.

Cong, Y., G. T. Banta, H. Selck, D. Berhanu, E. Valsami-Jones, and V. E. Forbes. 2014. "Toxicity and Bioaccumulation of Sediment-Associated Silver Nanoparticles in the Estuarine Polychaete, *Nereis (Hediste) diversicolor*." *Aquatic Toxicology* 156: 106–115.

Coull, B. C. 1990. "Are Members of the Meiofauna Food for Higher Trophic Levels?" *Transactions of the American Microscopical Society* 109: 233–246.

Coull, B. C., and G. T. Chandler. 1992. "Pollution and Meiofauna: Field, Laboratory, and Mesocosm Studies." *Oceanography and Marine Biology: An Annual Review* 30:191–271.

Cox, A., P. Venkatachalam, S. Sahi, and N. Sharma. 2016. "Silver and Titanium Dioxide Nanoparticle Toxicity in Plants: A Review of Current Research." *Plant Physiology and Biochemistry* 107: 147–163.

Croteau, M.-N., S. K. Misra, S. N. Luoma, and E. Valsami-Jones. 2011. "Silver Bioaccumulation Dynamics in a Freshwater Invertebrate after Aqueous and Dietary Exposures to Nanosized and Ionic Ag." *Environmental Science & Technology* 45: 6600–6607.

Dahl, U., E. Gorokhova, and M. Breitholtz. 2006. "Application of Growth-Related Sublethal Endpoints in Ecotoxicological Assessments Using a Harpacticoid Copepod." *Aquatic Toxicology* 77: 433–438.

Domingos, R. F., M. A. Baalousha, J. U. Y. Nam, M. M. Reid, N. Tufenki, J. R. Lead, G. G. Leppard, and K. J. Wilkinson. 2009. "Characterizing Manufactured Nanoparticles in the Environment: Multimethod Determination of Particle Sizes." *Environmental Science & Technology* 43: 7277–7284.

Fabrega, J., S. R. Fawcett, J. C. Renshaw, and J. R. Lead. 2009. "Silver Nanoparticle Impact on Bacterial Growth: Effect of pH, Concentration, and Organic Matter." *Environmental Science & Technology* 43: 7285–7290.

Ferson, S., L. Ginzburg, and A. Silvers. 1989. "Extreme Event Risk Analysis for Age-Structured Populations." *Ecological Modelling* 47: 175–187.

Foldbjerg, R., P. Olesen, M. Hougaard, D. A. Dang, H. J. Hoffmann, and H. Autrup. 2009. "PVP-Coated Silver Nanoparticles and Silver Ions Induce Reactive Oxygen Species, Apoptosis and Necrosis in THP-1 Monocytes." *Toxicology Letters* 190: 156–162.

Franci, G., A. Falanga, S. Galdiero, L. Palomba, M. Rai, G. Morelli, and M. Galdiero. 2015. "Silver Nanoparticles as Potential Antibacterial Agents." *Molecules* 20: 8856–8874.

Gee, J. 1989. "An Ecological and Economic Review of Meiofauna as Food for Fish." *Zoological Journal of the Linnean Society* 96: 243–261.

Giere, O. 2009. *Meiobenthology: The Microscopic Motile Fauna of Aquatic Sediments*. Berlin: Springer-Verlag.

Gottschalk, F., E. Kost, and B. Nowack. 2013. "Engineered Nanomaterials in Water and Soils: A Risk Quantification Based on Probabilistic Exposure and Effect Modeling." *Environmental Toxicology and Chemistry* 32: 1278–1287.

Green, A. S., and G. T. Chandler. 1996. "Life-Table Evaluation of Sediment-Associated Chlorpyrifos Chronic Toxicity to the Benthic Copepod, *Amphiascus tenuiremis*." *Archives of Environmental Contamination and Toxicology* 31: 77–83.

Griffitt, R. J., J. Luo, J. Gao, J.-C. Bonzongo, and D. S. Barber. 2008. "Effects of Particle Composition and Species on Toxicity of Metallic Nanomaterials in Aquatic Organisms." *Environmental Toxicology and Chemistry* 27: 1972–1978.

Gunsolus, I. L., M. P. S. Mousavi, K. Hussein, P. Bühlmann, and C. L. Haynes. 2015. "Effects of Humic and Fulvic Acids

on Silver Nanoparticle Stability, Dissolution, and Toxicity." *Environmental Science & Technology* 49: 8078–8086.

Hicks, G. R. F., and B. C. Coull. 1983. "The Ecology of Marine Meiobenthic Harpacticoid Copepods." *Oceanography and Marine Biology: An Annual Review* 21:67–175.

Hoecke, K. V., J. T. K. Quik, J. Mankiewicz-Boczek, K. A. C. D. Schamphealaere, A. Elsaesser, P. V. D. Meeren, C. Barnes, G. McKerr, C. V. Howard, and D. V. D. Meent. 2009. "Fate and Effects of CeO₂ Nanoparticles in Aquatic Ecotoxicity Tests." *Environmental Science & Technology* 43:4537–4546.

Hook, S. E., and N. S. Fisher. 2001. "Sublethal Effects of Silver in Zooplankton: Importance of Exposure Pathways and Implications for Toxicity Testing." *Environmental Toxicology and Chemistry* 20: 568–574.

Hutchins, D. A., W.-X. Wang, and N. S. Fisher. 1995. "Copepod Grazing and the Biogeochemical Fate of Diatom Iron." *Limnology and Oceanography* 40: 989–994.

Ivask, A., I. Kurvet, K. Kasemets, I. Blinova, V. Arujoa, S. Suppi, H. Vija, et al. 2014. "Size-Dependent Toxicity of Silver Nanoparticles to Bacteria, Yeast, Algae, Crustaceans and Mammalian Cells in Vitro." *PLoS ONE* 9: e102108.

Kim, K. T., L. Truong, L. Wehmas, and R. L. Tanguay. 2013. "Silver Nanoparticle Toxicity in the Embryonic Zebrafish Is Governed by Particle Dispersion and Ionic Environment." *Nanotechnology* 24: 115101.

Kwok, K. W. H., W. Dong, S. M. Marinakos, J. Liu, A. Chilkoti, M. R. Wiesner, M. Chernick, and D. E. Hinton. 2016. "Silver Nanoparticle Toxicity Is Related to Coating Materials and Disruption of Sodium Concentration Regulation." *Nanotoxicology* 10: 1306–1317.

Lang, K. 1948. *Monographie der Harpacticiden*. Koenigstein, West Germany: Otto Koeltz Science Publishers.

Leslie, P. H. 1945. "On the Use of Matrices in Certain Population Mathematics." *Biometrika* 33: 183–212.

Lotufo, G. R. 1997. "Toxicity of Sediment-Associated PAHs to an Estuarine Copepod: Effects on Survival, Feeding, Reproduction and Behavior." *Marine Environmental Research* 44: 149–166.

Lu, W., D. Senapati, S. Wang, O. Tovmachenko, A. K. Singh, H. Yu, and P. C. Ray. 2010. "Effect of Surface Coating on the Toxicity of Silver Nanomaterials on Human Skin Keratinocytes." *Chemical Physics Letters* 487: 92–96.

Navarro, E., A. Behra, R. Behra, N. B. Hartmann, J. Filser, A.-J. Miao, A. Quigg, P. H. Santschi, and L. Sigg. 2008. "Environmental Behavior and Ecotoxicity of Engineered Nanoparticles to Algae, Plants, and Fungi." *Ecotoxicology* 17: 372–386.

Navarro, E., B. Wagner, N. Odzak, L. Sigg, and R. Behra. 2015. "Effects of Differently Coated Silver Nanoparticles on the Photosynthesis of *Chlamydomonas reinhardtii*." *Environmental Science & Technology* 49: 8041–8047.

Newton, K. M., H. L. Puppala, C. L. Kitchens, V. L. Colvin, and S. J. Klaine. 2013. "Silver Nanoparticle Toxicity to *Daphnia magna* Is a Function of Dissolved Silver Concentration." *Environmental Toxicology and Chemistry* 32: 2356–2364.

OECD. 2014. *New Guideline for the Testing of Chemicals: New Guidance Document on Harpacticoid Copepod Development and Reproduction Test with *Amphiascus tenuiremis**. Paris: OECD publisher.

Power, M., and G. Power. 1995. "A Modelling Framework for Analyzing Anthropogenic Stresses on Brook Trout (*Salvelinus fontinalis*) Populations." *Ecological Modelling* 80: 171–185.

Raikhel, A. S., and T. S. Dhadialla. 1992. "Accumulation of Yolk Proteins in Insect Oocytes." *Annual Review of Entomology* 37: 217–251.

Reinfeldter, J. R., and N. S. Fisher. 1991. "The Assimilation of Elements Ingested by Marine Copepods." *Science* 251 (4995): 794–796.

Romer, I., T. A. White, M. Baalousha, K. Chipman, M. R. Viant, and J. R. Lead. 2011. "Aggregation and Dispersion of Silver Nanoparticles in Exposure Media for Aquatic Toxicity Tests." *Journal of Chromatography A* 1218: 4226–4233.

Shafir, S., M. Tom, M. Ovadia, and E. Lubzens. 1992. "Protein, Vitellogenin, and Vitellin Levels in the Hemolymph and Ovaries during Ovarian Development in *Penaeus semisulcatus* (De Haan)." *The Biological Bulletin* 183: 394–400.

Sikder, M., J. R. Lead, G. T. Chandler, and M. Baalousha. 2017. "A Rapid Approach for Measuring Silver Nanoparticle Concentration and Dissolution in Seawater by UV-Vis." *Science of the Total Environment* 618:597–607.

Stensberg, M. C., R. Madangopal, G. Yale, Q. Wei, O. C. H. O. A. H. Acuña, A. Wei, E. S. Mcclamore, J. Rickus, D. M. Porterfield, and M. S. Sepúlveda. 2014. "Silver Nanoparticle-Specific Mitotoxicity in *Daphnia magna*." *Nanotoxicology* 8: 833–842.

Sørensen, S. N., and A. Baun. 2015. "Controlling Silver Nanoparticle Exposure in Algal Toxicity Testing – A Matter of Timing." *Nanotoxicology* 9: 201–209.

Tejamaya, M., I. Romer, R. C. Merrifield, and J. R. Lead. 2012. "Stability of Citrate, PVP, and PEG Coated Silver Nanoparticles in Ecotoxicology Media." *Environmental Science & Technology* 46: 7011–7017.

Templeton, R. C., P. L. Ferguson, K. M. Washburn, W. A. Scrivens, and G. T. Chandler. 2006. "Life-Cycle Effects of Single-Walled Carbon Nanotubes (SWNTs) on an Estuarine Meiobenthic Copepod." *Environmental Science & Technology* 40: 7387–7393.

Vance, M. E., T. Kuiken, E. P. Vejerano, S. P. McGinnis, M. F. Hochella, J. R. D. Rejeski, and M. S. Hull. 2015. "Nanotechnology in the Real World: Redeveloping the Nanomaterial Consumer Products Inventory." *Beilstein Journal of Nanotechnology* 6: 1769–1780.

Vanhaecke, F., H. Vanhoe, R. Dams, and C. Vandecasteele. 1992. "The Use of Internal Standards in ICP-MS." *Talanta* 39 (7): 737–742.

Wei, L., J. Lu, H. Xu, A. Patel, Z.-S. Chen, and G. Chen. 2015. "Silver Nanoparticles: Synthesis, Properties, and Therapeutic Applications." *Drug Discovery Today* 20: 595–601.

Xu, Y., and W. X. Wang. 2004. "Silver Uptake by a Marine Diatom and Its Transfer to the Coastal Copepod *Acartia spinicauda*." *Environmental Toxicology and Chemistry* 23 (3): 682–690.

Yue, Y., R. Behra, L. Sigg, P. Fernández Freire, S. Pillai, and K. Schirmer. 2015. "Toxicity of Silver Nanoparticles to a Fish

Gill Cell Line: Role of Medium Composition." *Nanotoxicology* 9 (1): 54–63.

Yue, Y., R. Behra, L. Sigg, and K. Schirmer. 2016. "Silver Nanoparticles Inhibit Fish Gill Cell Proliferation in Protein-Free Culture Medium." *Nanotoxicology* 10: 1075–1083.

Zhu, X., L. Zhu, Y. Lang, and Y. Chen. 2008. "Oxidative Stress and Growth Inhibition in the Freshwater Fish *Carassius auratus* Induced by Chronic Exposure to Sublethal Fullerene Aggregates." *Environmental Toxicology and Chemistry* 27: 1979–1985.